

## Analytical Study on The Effect of Optical Filtration and Nano-PCM on The Performance of PV/T Solar Collectors

Ahmed S. Abd-Elrazik<sup>1,4</sup>, FA Al-Sulaiman<sup>1,2\*</sup>, Saidur R.<sup>2,3</sup>, and R Ben-Mansour<sup>1</sup>

<sup>1</sup> Mechanical Engineering Department, King Fahd University of Petroleum and Minerals, Dhahran, Saudi Arabia

<sup>2</sup> Center of Research Excellence in Renewable Energy (CoRERE), King Fahd University of Petroleum and Minerals, Dhahran, Saudi Arabia

<sup>3</sup> Research Centre for Nano-Materials and Energy Technology (RCNMET), School of Science and Technology, Sunway University, Malaysia

<sup>4</sup> Mechanical Power Engineering Department, Ain Shams University, Cairo (Egypt)

\*Corresponding Author: [fahadas@kfupm.edu.sa](mailto:fahadas@kfupm.edu.sa), Tel: +966 (13) 860-4628.

### Abstract

High temperature is a challenging problem with all solar collectors that are using PV panels for electricity production. Cooling of PV panels using traditional fluids become not effective as for the poor thermal properties of these fluids. Dispersion of nanoparticles with different liquid was found to enhance the thermal properties of these liquids. Nanofluids and Nano-Phase Change Materials (Nano-PCMs) were considered as promising solutions to enhance the performance of PV/Thermal (PV/T) systems. Nanofluids can be used beneath the PV for cooling or above it for optical filtration. In addition, Nano-PCM can be used beneath the PV for cooling and storage. In this study, an analytical solution was developed to evaluate the effect of using nanofluid filtration and nano-PCM on the overall performance of the PV/T solar collector. Four models were examined alternating between the presence and absence of optical filtration and lower nano-PCM layer. Neglecting the storage side, it was found that without optical filtration, presence of nano-PCM below the PV module decreases the overall efficiency (thermal + electrical) by around 6.7%. In contrast, presence of optical filtration decreases this percentage to be less than 1%. Moreover, using the optical filtration alone improves the overall efficiency by 6-12%.

*Keywords: Nanofluid, PCM, PV/Thermal, PV cooling, Optical filtration*

---

### 1. Introduction

Solar energy is considered one of the most promising sources of renewable energies that should be used efficiently to be able to completely replace the fossil fuel energy very soon. Many devices are used for the collection process of solar radiation. Hybrid Photovoltaic/Thermal collectors are found to combine the advantages of electrical and thermal energy generation as well as solving the problem of performance degradation of PV cells because of high temperature by cooling the PV panels. In this demand, many researches had been made alternating from changing the design of the collector to using different cooling fluids to attain the highest possible overall efficiency.

Hussain et al. (2013) studied the efficiency of using honeycomb channels beneath the PV in enhancing the thermal efficiency of hybrid PV/T collector cooled by air. They examined the enhancement under different flow rates. It was found the thermal efficiency enhanced from 27% to 87% when using honeycomb channels with air mass flow rate of 0.11 kg/s. Fudholi et al. (2014) investigated a study for different configurations of water cooled PV/T under different mass flow rates and solar irradiation levels. Three different new absorber channels were proposed; web flow absorber, direct flow absorber, and spiral flow absorber. They found that as the mass flow rate increases, the PV temperature decreases and the electrical efficiency increases. Also, increasing the solar radiation level increases the PV temperature and the generated electrical efficiency. They ended up with that the spiral flow absorber presented

the highest overall performance at solar incident radiation of 800 W/m<sup>2</sup>, with overall, thermal, and electrical efficiencies of 68.4, 54.6, and 13.8% respectively.

Nanofluids, which was first proposed by Choi and Eastman (1995), for enhancing the thermal properties of different fluids were used for the cooling purposes of the PV module as well as collecting the large possible amount of heat from solar radiation. Nanofluids were used in channels below the PV module (H Zhu and C Zhang, 2006; A Kasaeian et al., 2015; W I.A.Aly, 2014) and were recently used to flow in the front of the PV module for optical filtration (N. E. Hjerrild et al., 2016) beside the cooling objective. Vakili et al. (2016) examined the effect of using graphene nanoplatelets in enhancing the heat transfer in solar collectors as it is dispersed in a deionized water as a base fluid. The authors tried different concentration in weight fractions of 0.0005, 0.001, and 0.005, and different mass flow rates of 0.0075, 0.015, and 0.225 kg/s. Maximum efficiency was obtained at mass flow rate of 0.015 kg/s and there was an enhancement in the thermal efficiency with increasing the concentration of the nanoparticles. Hajjar et al. (2014) proposed a study on the thermal conductivity enhancement as a result of using graphene oxide nanofluids. Through all types of GO/water nanofluids, GO 5 had the best enhancement in thermal conductivity relative to that of water (about 47.54% more than water at 40°C). In addition, regarding its optical properties, they examined high absorbance for the graphene oxide nanofluid in the spectral range of solar radiation. Hassani et al. (2016a, 2016b) used nanofluid as spectrally-selective material for the solar irradiation. They found that the nanofluid-optical filter did not prevent solar radiation from reaching the PV panels, and at the same time, it gets the most benefit from the solar thermal energy. Moreover, silver/water nanofluid was found to be better than only water, as water alone is not capable of absorbing except the IR spectra.

As the solar radiation is not constant throughout the day and the need for the availability of energy in the night time, it became necessary to have storage for the absorbed solar radiation. Phase Change Materials (PCMs) were found to be the best storage idea with solar collectors, as it has very high capacity and it makes cooling as well. In contrast, low thermal conductivity of PCM causes a resistance for heat transfer so dispersing some nanoparticles for enhancement of thermal conductivity was proposed reaching the Nano-PCMs concept. Colla et al. (2017) discussed the feasibility of using alumina and carbon black nanoparticles with pure paraffin waxes PCM. Two PCM materials were examined (RT20 and RT25) with the addition of nanoparticles (Carbon black and Aluminum oxide). They ended up with that the addition of alumina can make an enhancement in the latent heat while CB will be able to make an enhancement in the thermal conductivity that is required. Su et al. (2017) investigated a comparative study on the benefits behind using PCM in cooling the hybrid PV/T solar collectors. The effect of PCM position relative to the cooling channels on the surface temperature, outlet temperature and the efficiencies were studied as well as the effect of the thickness of the PCM layer. It was found that putting the PCM on the upper side of the duct with 3 cm thickness gives higher overall efficiency.

The current paper studies the effect of existence of optical filtration above the PV and PCM beneath the PV in enhancing the overall efficiency of the PV/T solar collector by studying four different models alternating between existence and absence of optical filtration and PCM layer. It was found that existence of optical filtration above the PV and absence of PCM layer beneath the PV will result in the best performance.

## 2. Method:

The analytical equations governing the energy transfer through the PV/T were developed. These equations included all the physical, optical, thermal, and electrical contributions of the system. A systematic study for the governing equations was studied under reasonable assumptions to examine the thermal and electrical performance of the PV/T under different configurations.

### 2.1. The physical model:

In this part, the physical descriptions of the different provided configurations (M-1 to M-4) are discussed. Model-1 consists of one PV module, one thermal unit below the PV for the cooling purposes at which water/graphene nanofluid is used, and one thermal above the PV for the optical filtration purposes at which water/silver is used. Also, single PCM layer under the PV with graphene nanoparticles for storage and cooling as well. Model-2 is the same as Model-1 but without nano-PCM layer at the bottom of PV. Model-3 is slightly different from Model-1 that the optical filtration was removed and a vacuum channel was added at the bottom of the cooling channels. Model-4 is exactly like Model-3 but also without using nano-PCM layer at the bottom of the PV panels. Figure 1 shows schematic

diagrams for the proposed designs for the PV/T solar collector.

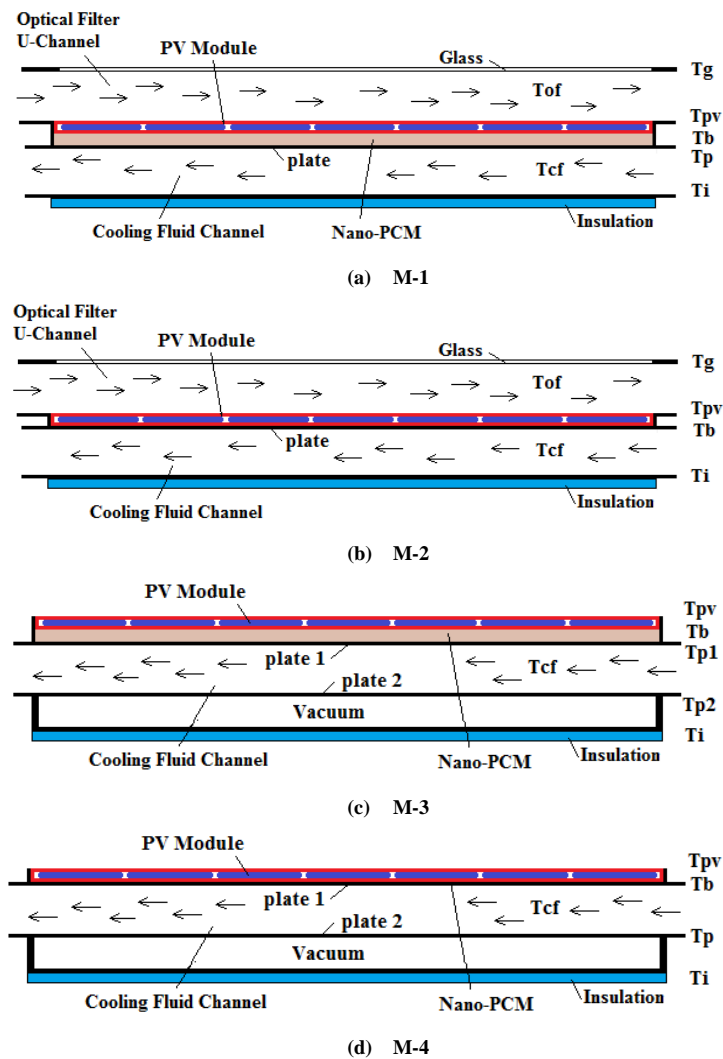


Figure 1 Numerical solution models

## 2.2. Working principles of PV/T configurations:

Figure 1-(a) shows the configuration of the first model M-1. In M-1, the incident solar radiation reaches the PV cells after passing through the first cover glass, then through the optical filtration fluid channel through. The optical filtration fluid is responsible for allowing the solar radiation within the useful spectral range for electricity production only to pass through. The nano-PCM layer at the bottom of the PV is responsible for storing heat as well as transferring heat to the cooling fluid beneath the PV module. Nanoparticles were added to the PCM layer to enhance its thermal conductivity. It was guessed that the nano-PCM layer may resist the heat transfer to the cooling fluid and that's why it was removed in M-2. In Model-3, the optical filtration was removed totally and the solar radiation reached the PV cells directly. In M-4 the nano-PCM layer was also removed.

## 2.3. Mathematical model:

The simple general numerical models presented later were used to evaluate the performance of the PV/T collector through the calculation of the different temperatures, thermal, and electrical efficiencies using previously calculated optical and thermal properties. Table 1 shows the governing equations for the four proposed models. The assumptions that were used in this study are listed in Table 2. In addition, the technical data of the proposed models are available

at Table 3. The optical properties for the optical filter were taken from literature [10,11]. Table 4 summarize the thermal and rheological properties of the main substances used in the models.

**Table 1 Governing equations for the proposed Models**

| M- # | Balance       | Governing Equations   | Equation no. |
|------|---------------|---|--------------|
| 1    | Glass cover   | $\alpha_g G = h_{g-am}(T_g - T_{am}) + h_{g-of}(T_g - \bar{T}_{of})$  | (eq. 1)      |
|      | Optical fluid | $\tau_g \alpha_{of} G = h_{of-g}(\bar{T}_{of} - T_g) + h_{of-pv}(\bar{T}_{of} - T_{pv}) + \frac{m^o_{of} c p_{of}}{W} \frac{dT_{of}}{dx_1}$ | (eq. 2)      |
|      | PV panel      | $\alpha_{pv} \tau_g \tau_{of} G = h_{pv-of}(T_{pv} - \bar{T}_{of}) + \frac{T_{pv} - T_b}{R_b} + \eta_c \alpha_{pv} \tau_g \tau_{of} G$      | (eq. 3)      |
|      | Back plate    | $\frac{T_{pv} - T_b}{R_b} = k_{PCM} \frac{T_b - T_{p1}}{\Delta t_{PCM}}$  | (eq. 4)      |
|      | Plate 1       | $k_{PCM} \frac{T_b - T_p}{\Delta t_{PCM}} = h_{p-cf}(T_p - \bar{T}_{cf})$   | (eq. 5)      |
|      | Cooling fluid | $h_{p-cf}(T_p - \bar{T}_{cf}) = h_{cf-l}(\bar{T}_{cf} - T_l) + \frac{m^o_{cf} c p_{cf}}{L} \frac{dT_{cf}}{dx_2}$                            | (eq. 6)      |
|      | Insulation    | $h_{cf-l}(\bar{T}_{cf} - T_l) = h_{l-am}(T_l - T_{am})$   | (eq. 7)      |
|      | Efficiency    | $\eta_c = \eta_{ref}[1 - \beta_{ref}(T_c - T_{ref})]$   | (eq. 8)      |
| 2    | Glass cover   | $\alpha_g G = h_{g-am}(T_g - T_{am}) + h_{g-of}(T_g - \bar{T}_{of})$  | (eq. 9)      |
|      | Optical fluid | $\tau_g \alpha_{of} G = h_{of-g}(\bar{T}_{of} - T_g) + h_{of-pv}(\bar{T}_{of} - T_{pv}) + \frac{m^o_{of} c p_{of}}{W} \frac{dT_{of}}{dx_1}$ | (eq. 10)     |
|      | PV panel      | $\alpha_{pv} \tau_g \tau_{of} G = h_{pv-of}(T_{pv} - \bar{T}_{of}) + \frac{T_{pv} - T_b}{R_b} + \eta_c \alpha_{pv} \tau_g \tau_{of} G$      | (eq. 11)     |
|      | Back plate    | $\frac{T_{pv} - T_b}{R_b} = h_{p-cf}(T_b - \bar{T}_{cf})$   | (eq. 12)     |
|      | Cooling fluid | $h_{p-cf}(T_b - \bar{T}_{cf}) = h_{cf-l}(\bar{T}_{cf} - T_l) + \frac{m^o_{cf} c p_{cf}}{L} \frac{dT_{cf}}{dx_2}$                            | (eq. 13)     |
|      | Insulation    | $h_{cf-l}(\bar{T}_{cf} - T_l) = h_{l-am}(T_l - T_{am})$   | (eq. 14)     |
|      | Efficiency    | $\eta_c = \eta_{ref}[1 - \beta_{ref}(T_c - T_{ref})]$   | (eq. 15)     |
| 3    | PV panel      | $\alpha_g G = h_{pv-am}(T_{pv} - T_{am}) + \frac{T_{pv} - T_b}{R_b} + \eta_c \alpha_g G$  | (eq. 16)     |
|      | Back plate    | $\frac{T_{pv} - T_b}{R_b} = k_{PCM} \frac{T_b - T_{p1}}{\Delta t_{PCM}}$  | (eq. 17)     |
|      | Plate 1       | $k_{PCM} \frac{T_b - T_{p1}}{\Delta t_{PCM}} = h_{p1-cf}(T_{p1} - \bar{T}_{cf})$  | (eq. 18)     |
|      | Cooling fluid | $h_{p1-cf}(T_{p1} - \bar{T}_{cf}) = h_{cf-p}(\bar{T}_{cf} - T_{p2}) + \frac{m^o_{cf} c p_{cf}}{L} \frac{dT_{cf}}{dx_2}$                     | (eq. 19)     |
|      | Plate 2       | $h_{cf-p2}(\bar{T}_{cf} - T_{p2}) = h_{r,p2-l}(T_{p2} - T_l)$   | (eq. 20)     |
|      | Insulation    | $h_{r,p2-l}(T_{p2} - T_l) = h_{l-am}(T_l - T_{am})$   | (eq. 21)     |
|      | Efficiency    | $\eta_c = \eta_{ref}[1 - \beta_{ref}(T_c - T_{ref})]$   | (eq. 22)     |
| 4    | PV panel      | $\alpha_g G = h_{pv-am}(T_{pv} - T_{am}) + \frac{T_{pv} - T_b}{R_b} + \eta_c \alpha_g G$  | (eq. 23)     |
|      | Back plate    | $\frac{T_{pv} - T_b}{R_b} = h_{b-cf}(T_b - \bar{T}_{cf})$   | (eq. 24)     |
|      | Cooling fluid | $h_{b-cf}(T_b - \bar{T}_{cf}) = h_{cf-p}(\bar{T}_{cf} - T_p) + \frac{m^o_{cf} c p_{cf}}{L} \frac{dT_{cf}}{dx_2}$                            | (eq. 25)     |
|      | Plate         | $h_{cf-p}(\bar{T}_{cf} - T_p) = h_{r,p-l}(T_p - T_l)$   | (eq. 26)     |

|            |   |          |
|------------|---|----------|
| Insulation | $h_{r,p-l}(T_p - T_l) = h_{l-am}(T_l - T_{am})$       | (eq. 27) |
| Efficiency | $\eta_c = \eta_{ref}[1 - \beta_{ref}(T_c - T_{ref})]$ | (eq. 28) |

**Table 2 Assumptions considered in the present study**

| Assumptions |  |
|-------------|--|
| 1           | Steady state   |
| 2           | Normal incident radiation  |
| 3           | Radiation losses from glass cover or insulation to atmosphere were neglected |
| 4           | Very thin glass covers, plates, and insulation so conduction was neglected   |
| 5           | Working fluid is flowing through a rectangular channel                       |
| 6           | Heat transfer was only considered in one dimension                           |
| 7           | All fluids remain liquids through the operation of the system                |
| 8           | Thermal properties were calculated at an average temperature of 30°C         |
| 9           | Negligible pumping power due to very low mass flow rate                      |
| 10          | Reference electrical efficiency of 12%                                       |

**Table 3 Technical design data of the different solar collectors investigated in the present study**

| Item           | Specifications   | M-1 | M-2 | M-3 | M-4 |
|----------------|--|-----|-----|-----|-----|
| Glass cover-1  | $\tau_g = 0.9$<br>$\alpha_g = 0.05$  | √   | √   | √   | √   |
| Optical filter | Nanofluid, water/silver [11]<br>$\tau_{of} = 0.62$<br>$\alpha_{of} = 0.38$ | √   | √   |     |     |
| Glass cover-2  | $\tau_g = 0.9$<br>$\alpha_g = 0.05$  | √   | √   |     |     |
| PV cell        | Multi-crystalline<br>$\alpha_g = 0.945$                                    | √   | √   | √   | √   |
| Back-plate     |  | √   | √   | √   | √   |
| Nano-PCM       | PCM/graphene   | √   |     | √   |     |
| Plate-1        |  | √   |     | √   |     |
| Working fluid  | Nanofluid, water/graphene  | √   | √   | √   | √   |
| Plate-2        | $\varepsilon_p = 0.9$  | √   | √   | √   | √   |
| Vacuum         |  |     |     | √   | √   |
| Insulation     |  | √   | √   | √   | √   |

**Table 4 Thermal and rheological properties**

| Substance/Property | k        | μ                       | ρ        | C <sub>p</sub> |
|--------------------|----------|-------------------------|----------|----------------|
| Air                | 0.026424 | 18.718×10 <sup>-6</sup> | 1.165285 | 1007.22        |
| Water              | 0.615504 | 0.000797345             | 995.65   | 4180.02        |
| PCM                | 0.195    | 0.01145                 | 820      | 2500           |
| Graphene           | 5000     | -                       | 1000     | 15             |
| Silver             | 429      | -                       | 10500    | 235            |

## 2.4. Thermal and rheological properties of nanofluids and nano-PCM:

The equivalent thermal properties for the nanofluids and nano-PCM were calculated based on the formulas that are available in the literature.

Thermal conductivity:

$$k_{nf} = \left[ \frac{k_p + 2k_f - 2\phi(k_f - k_p)}{k_p + 2k_f + \phi(k_f - k_p)} \right] k_f \quad (\text{eq. 29})$$

Dynamic viscosity:

$$\mu_{nf} = \frac{1}{(1-\phi)^{2.5}} \mu_f \quad (\text{eq. 30})$$

Density:

$$\rho_{nf} = \phi\rho_p + (1 - \phi)\rho_f \quad (\text{eq. 31})$$

Specific heat:

$$(\rho c_p)_{nf} = \phi(\rho c_p)_p + (1 - \phi)(\rho c_p)_f \quad (\text{eq. 32})$$

Table 5 shows the thermal and rheological properties of the nanofluids and nano-PCM used in the present study.

**Table 5 Properties of Nanofluids and nano-PCM**

|                | $\phi$ | $\mu$  | $\rho$    | $c_p$    | $k$     |
|----------------|--------|--------|-----------|----------|---------|
| Optical filter | 0.001  | 0.0008 | 1005.1543 | 4138.8   | 0.61734 |
| Working fluid  | 0.001  | 0.0008 | 995.65    | 4175.855 | 0.61735 |
| Nano-PCM       | 0.001  | -      | 820.18    | -        | 0.19558 |

## 2.5. Temperature distribution::

In the current section, the equations describing the temperature distribution throughout the optical filtration and cooling nanofluids used with M-1 were formulated. The energy equations that communicate between the fluids temperatures and its surroundings were used.

The working fluid:

From eq. 6:

$$h_{p-cf}(T_p - \bar{T}_{cf}) = h_{cf-l}(\bar{T}_{cf} - T_l) + \frac{m^o_{cf} c_{p_{cf}}}{L} \frac{dT_{cf}}{dx_2}$$

By rearranging,

$$\therefore \frac{dT_{cf}}{dx_2} = \frac{L}{m^o_{cf} c_{p_{cf}}} [h_{p-cf}(T_p - T_{cf}) - h_{cf-l}(T_{cf} - T_l)]$$

$$\therefore \frac{dT_{cf}}{dx_2} = \frac{L}{m^o_{cf} c_{p_{cf}}} [h_{p-cf}T_p + h_{cf-l}T_l - T_{cf}(h_{p-cf} + h_{cf-l})]$$

$$\text{Take } A = \frac{L}{m^o_{cf} c_{p_{cf}}} (h_{p-cf}T_p + h_{cf-l}T_l), B = \frac{L}{m^o_{cf} c_{p_{cf}}} (h_{p-cf} + h_{cf-l})$$

$$\therefore \frac{dT_{cf}}{dx_2} = A - BT_{cf}$$

$$\int_{T_{cf,in}}^{T_{cf,x2}} \frac{dT_{cf}}{A - BT_{cf}} = \int_0^{x_2} dx_2$$

$$\therefore T_{cf}(x_2) = \frac{A}{B} - \left[ \frac{A}{B} - T_{cf,in} \right] \exp(-Bx_2) \quad (\text{eq. 33})$$

$$T_{cf}(W) = \frac{A}{B} - \left[ \frac{A}{B} - T_{cf,in} \right] \exp(-BW) \quad (\text{eq. 34})$$

$$\bar{T}_{cf} = \frac{1}{W} \int_0^W T_{cf}(x_2) dx_2 = \frac{1}{W} \int_0^W \left[ \frac{A}{B} - \left[ \frac{A}{B} - T_{cf,in} \right] \exp(-Bx_2) \right] dx_2$$

$$\therefore \bar{T}_{cf} = \frac{A}{B} - \frac{1}{B^2W} [A - BT_{cf,in}] [\exp(-BW) - 1] \quad (\text{eq. 35})$$

The optical filter channel:

From eq. 2:

$$\tau_g \alpha_{of} G = h_{of-g} (\bar{T}_{of} - T_g) + h_{of-pv} (\bar{T}_{of} - T_{pv}) + \frac{m^o_{of} c p_{of}}{W} \frac{dT_{of}}{dx_1}$$

By rearranging,

$$\therefore \frac{dT_{of}}{dx_1} = \frac{W}{m^o_{of} c p_{of}} [\tau_g \alpha_{of} G - h_{of-g} (T_{of} - T_g) - h_{of-pv} (T_{of} - T_{pv})]$$

$$\therefore \frac{dT_{of}}{dx_1} = \frac{W}{m^o_{of} c p_{of}} [\tau_g \alpha_{of} G + h_{of-g} T_g + h_{of-pv} T_{pv} - T_{of} (h_{of-g} + h_{of-pv})]$$

$$\text{Take } C = \frac{W}{m^o_{of} c p_{of}} [\tau_g \alpha_{of} G + h_{of-g} T_g + h_{of-pv} T_{pv}], D = \frac{W}{m^o_{of} c p_{of}} (h_{of-g} + h_{of-pv})$$

$$\therefore \frac{dT_{of}}{dx_1} = C - DT_{of}$$

$$\int_{T_{of,in}}^{T_{of,x1}} \frac{dT_{of}}{C - DT_{of}} = \int_0^{x_1} dx_1$$

$$\therefore T_{of}(x_1) = \frac{C}{D} - \left[ \frac{C}{D} - T_{of,in} \right] \exp(-Dx_1) \quad (\text{eq. 36})$$

$$T_{of}(L) = \frac{C}{D} - \left[ \frac{C}{D} - T_{of,in} \right] \exp(-DL) \quad (\text{eq. 37})$$

$$\bar{T}_{of} = \frac{1}{L} \int_0^L T_{of}(x_1) dx_1 = \frac{1}{L} \int_0^L \left[ \frac{C}{D} - \left[ \frac{C}{D} - T_{of,in} \right] \exp(-Dx_1) \right] dx_1$$

$$\therefore \bar{T}_{of} = \frac{C}{D} - \frac{1}{D^2L} [C - DT_{of,in}] [\exp(-DL) - 1] \quad (\text{eq. 38})$$

Table 6 Reference values used

|  |       |                               |        |
|--|-------|-------------------------------|--------|
| <b>L (cm)</b>                            | 103.5 | <b>T<sub>wf, in</sub> (K)</b> | 298    |
| <b>W (cm)</b>                            | 100   | <b>T<sub>of, in</sub> (K)</b> | 298    |
| <b>L<sub>c</sub> (cm)</b>                | 100   | <b>V<sub>am</sub> (m/s)</b>   | 1      |
| <b>Δt<sub>PCM</sub> (cm)</b>             | 0.5   | <b>m<sup>o</sup> (kg/s)</b>   | 0.0104 |
| <b>Working fluid channel width (cm)</b>  | 4     | <b>η<sub>ref</sub> (%)</b>    | 12     |
| <b>Optical filter channel width (cm)</b> | 2     | <b>β</b>                      | 0.0045 |
| <b>T<sub>am</sub> (K)</b>                | 298   |                               |        |

## 2.6. Calculation of heat transfer coefficients for M-1:

For flow over flat plate surfaces,  $Nu = 0.86Re^{1/3}Pr^{1/2}$ ,  $Re = \frac{\rho v L_c}{\mu} \Big|_{am}$ ,  $Pr = \frac{\mu c_p}{k} \Big|_{am}$

Using the properties of air mentioned before and that  $h = \frac{Nu k_{am}}{L_c}$

$$h_{g-am} = h_{l-am} = 5.065 \text{ W/m.K}$$

For internal laminar flow with constant heat flux inside rectangular channels, and with height to width > 8,  $Nu = 8.24$ ,

Then for the optical filter fluid,  $h = \frac{Nu k_{of}}{D_{h,of}}$

With  $D_{h,of} = 3.92$  cm, and the properties of the optical filter nanofluid,

$$h_{g1-of} = h_{g2-of} = h_{p2-of'} = h_{l-of'} = 129.715 \text{ W/m.K}$$

And for the working fluid,  $h = \frac{Nu k_{wf}}{D_{h,wf}}$

With  $D_{h,wf} = 7.69$  cm, and the properties of the working fluid nanofluid,

$$h_{p1-wf} = h_{p2-wf} = 66.13 \text{ W/m.K}$$

## 3. Analytical results and discussion

The governing equations were solved separately for each model and the results are shown in Figure 2, Figure 3, Figure 4, and Figure 5. In addition, the results for solving the governing equations for conventional PV module were also discussed.

Studying the effect of existence of optical filtration, a comparison were held between the performance of models 1 and 2 versus that for models 3 and 4, it can be seen clearly that the existence of the optical filtration helped in enhancing the overall performance of the PV/T system. Comparing the models with optical filtration to the models without optical filtration, it was found that the PV temperature has decreased by 16-27.6 °C (Figure 2), electrical efficiency increased by 0.87-1.49% (Figure 3), and thermal efficiency increased by 11.7-17.4% (Figure 4).

The effect of the existence of the nano-PCM layer below the PV module can be distinguished by comparing the performance of M-1 with M-2 and M-3 with M-4. It was found that treating the nano-PCM on its thermal conductivity and neglecting its storage effects will end up with the result that existence of nano-PCM will decrease the performance due to low thermal conductivity and as a result resistance to heat transfer from the bottom side of the PV to the cooling fluid. Figure 2 to Figure 5 show that the effect of nano-PCM existence is not significant in the models that deal with optical filtration fluid; M-1 and M-2, M-3. In contrast, the effect of existence of nano-PCM layer in resisting the heat flow is very clear when comparing the performance of M-3 to M-4.



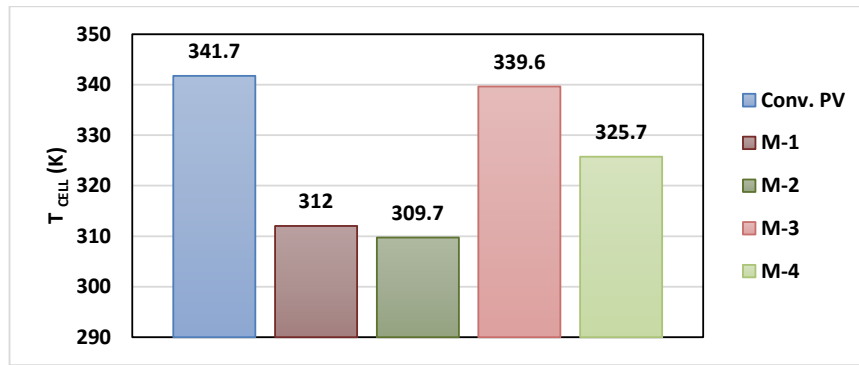


Figure 2 PV cell temperature for different models

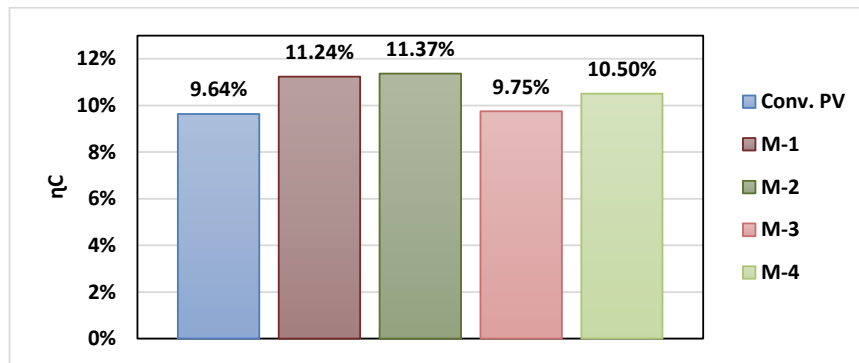


Figure 3 Electrical efficiency for different models

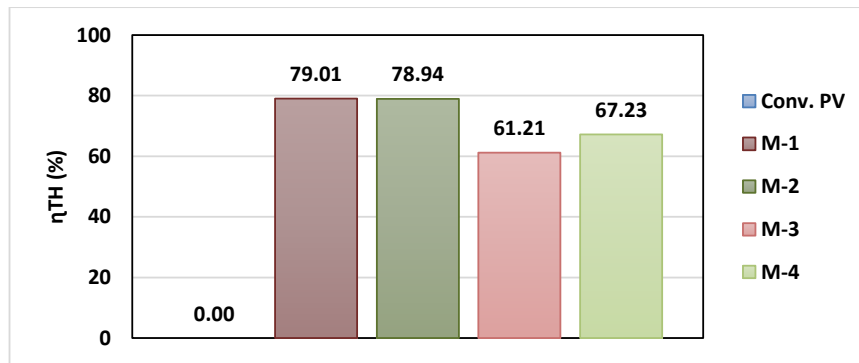


Figure 4 Thermal efficiency for different configurations

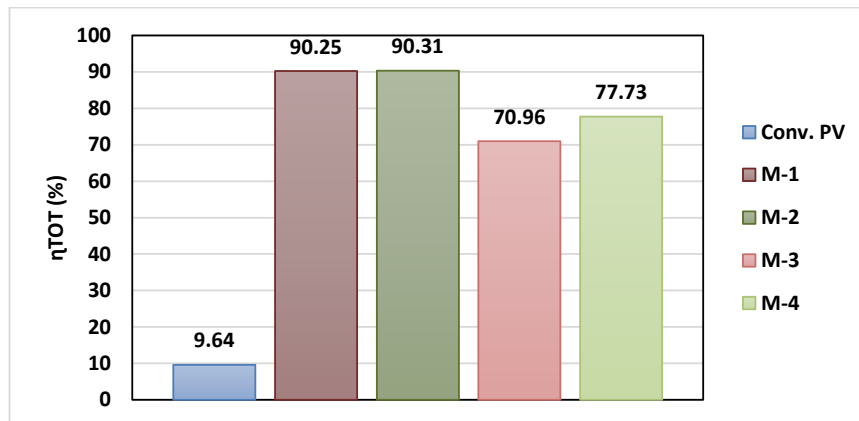


Figure 5 Total efficiency for different configurations

## 4. Conclusions

In the current paper, an analytical solution based on steady state assumption was developed. Four different models of hybrid PV/T solar systems studying the effect of optical filtration and nano-PCM technologies were studied. The governing energy equations for the heat transfer throughout the four models were solved to evaluate the solar utilization performance. From the discussion of the results, different conclusions were attained and can be summarized in:

- Using optical filtration is highly beneficial in enhancing the overall performance of PV/T systems.
- Neglecting the storage effect of the nano-PCM, existence of nano-PCM layer below the PV cells resists heat transfer to working fluid and thus increase the temperature of PV cells and decrease the performance of PV/T.

## 5. Additional work:

- Considering the honeycomb channels during analysis should end up with more enhancement in the performance of the PV/T.
- Using only one channel for optical filtration may increase or decrease the performance, so it needs to be studied.

## 6. References:

- Aly WI ,2014. Numerical study on turbulent heat transfer and pressure drop of nanofluid in coiled tube-in-tube heat exchangers. *Energy Convers Manage*;79:304–16.
- Choi SUS, Eastman JA, 1995. Enhancing thermal conductivity of fluids with nanoparticles. *ASME Int Mech Eng Congr Expo*;66:99–105.
- Colla L, Fedele L, Mancin S, Danza L, Manca O, 2017. Nano-PCMs for enhanced energy storage and passive cooling applications. *Appl Therm Eng*;110:584–9.
- Fudholi A, Sopian K, Yazdi MH, Hafidz M, Ibrahim A, Kazem HA, 2014. Performance analysis of photovoltaic thermal ( PVT ) water collectors. *Energy Convers Manag*;78:641–51.
- Haitao Zhua and Canying Zhang, 2006. Effects of nanoparticle clustering and alignment on thermal conductivities of Fe<sub>3</sub>O<sub>4</sub> aqueous nanofluids n.d. *Appl. Phys. Lett.* 89, 023123
- Hajjar Z, Rashidi A, Ghozatloo A, 2014. Enhanced thermal conductivities of graphene oxide nano fluids. *Int Commun Heat Mass Transf*;57:128–31.
- Hjerrild NE, Mesgari S, Crisostomo F, Scott JA, Amal R, Taylor RA, 2016. Hybrid PV/T enhancement using selectively absorbing Ag-SiO<sub>2</sub>/carbon nanofluids. *Sol Energy Mater Sol Cells*;147:281–7.
- Hussain F, Othman MYH, Yatim B, Ruslan H, Sopian K, Ibarahim Z, 2013. A study of PV/T collector with honeycomb heat exchanger. *AIP Conf Proc*;1571:10–6.
- Kasaeian A, Daviran S, Azarian RD, Rashidi A, 2015. Performance evaluation and nanofluid using capability study of a solar parabolic trough collector. *Energy Convers Manage*;89:368–75.
- Samir Hassani, Robert A. Taylor, Saad Mekhilef, R. Saidur, 2016a. A cascade nanofluid-based PV/T system with optimized optical and thermal properties. *Energy*;112:963–75.
- Samir Hassani, R. Saidur, Saad Mekhilef, Robert A. Taylor, 2016b. Environmental and exergy benefit of nanofluid-based hybrid PV/T systems. *Energy Convers Manag*;123:431–44.
- Su D, Jia Y, Alva G, Liu L, Fang G, 2017. Comparative analyses on dynamic performances of photovoltaic – thermal solar collectors integrated with phase change materials;131:79–89.
- Vakili M, Hosseinalipour SM, Delfani S, Khosrojerdi S, Karami M, 2016. Experimental investigation of graphene nanoplatelets nanofluid-based volumetric solar collector for domestic hot water systems. *Sol Energy*;131:119–30.